ELSEVIER

Proceedings of the JMSM 2008 Conference

Effect of heat treatment on plasticity of Al-Zn-Mg alloy: Microstructure evolution and mechanical properties

M. Chemingui[a,b]*, M. khitouni[a], G. Mesmacque[b] and A.W. Kolsi[a]

[a]Laboratoire de Chimie Inorganique(99/UR/12-22), FSS, B. P. 1171 – 3018, Sfax – Tunisia
[b]Laboratoire de mécanique de lille,Cité Scientifique 59650 Villeneuve d'Ascque- France.

Abstract

The effect of heat treatment on the plastic properties of an aluminum alloy (Al-Zn-Mg) has been investigated by indentation and tensile tests. The microstructural evolution was investigated using optical, scanning and transmission electron microscopies. After various states of ageing, the Al-Zn-Mg alloy shows significant changes in the microstructure and mechanical behaviour. After quenching, the microstructure was characterized by high ductility. After ageing at 135°C, corresponding to the maximum value of hardness, the alloy reveals small η' precipitates. After two-step ageing at 70°C plus at 135°C, the volume fraction of this precipitates becomes higher. Consequently, the yield strength of the material increases and it maintains its ductility.
© 2009 Elsevier B.V. Open access under CC BY-NC-ND license.

PACS: Type pacs here, separated by semicolons ;

Keywords: Al-Zn-Mg alloy; Precipitation hardening; Microstructure, Mechanical behaviour.

1. Introduction

Al-Zn-Mg alloys are used extensively in aerospace industry due to their ultrahigh strength as well as their low density. These alloys have also the advantage of being readily weldable. Their proprieties can be obtained through control of the precipitation hardening process. Age hardening of aluminium alloys has been investigated in the past few years. Therefore, many researches have been concentrated on the precipitation and on the related hardening of the alloys both from the experimental and theoretical viewpoint [1-7].

The decomposition of the supersaturated solid solution is known to take place via the formation of several phases which may precipitate simultaneously. Depending on thermal treatments, the unmixing processes can be described as follows [4, 8-10]:

α- Supersaturated Solid Solution (α-sss)→GP zones (Zn, Mg)→ metastable η'(Hex.)→ stable η(MgZn$_2$) (Hex.).

In most ternary Al-Zn-Mg alloys, maximum hardening occurs at aging temperatures up to ~130°C. Under these conditions, the microstructure consists mainly of GP zones and η' phases. It has been generally accepted that the intermediate precipitate η' nucleates from, or at the sites of these zones, although other work has suggested that this may not necessarily be so [11].

* Corresponding author. Tel.: +216-97-699-203; fax: +216-74-274-437.
E-mail address: chmingui_mahmoud@yahoo.fr.

Interactions between dislocations and solute atoms have been extensively studied for many years: in stable solid solution, the influence of elements on yield stress [12], work hardening [13-16] and dynamic strain ageing leading to plastic instabilities [17-18] have been thoroughly investigated. During tensile testing at room temperature after quenching (the purpose of which may be to relieve quench-related internal stresses), a variety of evidence indicates that similar dynamic precipitation may occur [19].

For the purpose of the alloy design, understanding the relationship between fracture behaviour and microstructure is a vital requirement. Fracture behaviour of Al-alloys is essentially controlled by the volume fractions and character of inclusions, dispersoids and precipitates. The micromechanisms governing fracture characteristics of age hardened alloys depend on coherency and distribution of precipitates, grain size and shape, grain boundary precipitates, the presence of other particles which result from impurities [20].

The yield stress and the ductility are known to be paradoxical: the maximum of age hardening corresponds to the minimum of ductility. Thus, the purpose of the present work is to check the heat treatment that offers a better compromise: after achieving a high yield strength, heat treatments can give rise also to an increase in ductility. Therefore, the study requires a complete characterization of the microstructure and of the mechanical behaviour in tensile and indentation tests.

2. Experimental

The material used in this study was the Al-Zn-Mg alloy. It was analyzed by inductively coupled plasma optical emission spectrometry (ICPOES). The chemical composition is given in Table 1. After solution treating of the alloy specimens at 475°C for 24 h and icy water quenching, a natural aging was performed for 3.5 days. Such preparation of samples allows us to observation of the evolution of the microstructure, i.e. the precipitation process and the study of the mechanical properties by means of indentation and tensile tests.

Table 1. Chemical composition of the investigated material (wt %).

Al	Zn	Mg	Cu	Mn	Fe	Si	Ti	Cr
Balance	4.6	1.2	0.065	0.3	0.25	0.23	0.036	0.18

Vickers microhardness (Hv) was measured on samples using shimadzu HVM-2000 hardness, at a load of 500g applied for 15 seconds. For Optical microscopy (OM) and scanning electron microscopy (SEM) investigations, the surfaces of specimens were mechanically grounded and chemical polished, using a mixture of 6% HNO_3, 4% HF, 10% H_3PO_4 and 80% H_2O. For the transmission electron microscopy (TEM) studies, thin foils were prepared by mechanical-polishing. They were examined in a JEM-2000FX transmission electron microscope operated at an accelerating voltage of 200 kV.

The tensile specimens were machined directly from the selected heat treated and quenched samples. The specimens have a gauge length of 70 mm, a gauge of width of 20 mm and a gauge thick of 6mm

3. Results and discussions

Figure 1 represents the microhadness evolution as a function of temperatures for the investigated alloy aged for 2 hours. Three specimens, A, B and C, were selected to determine the effect of heat treatment on strength and ductility of Al-Zn-Mg alloy. The position of each sample, with respect to the microhardness-temperature curves, is shown in figure 1.
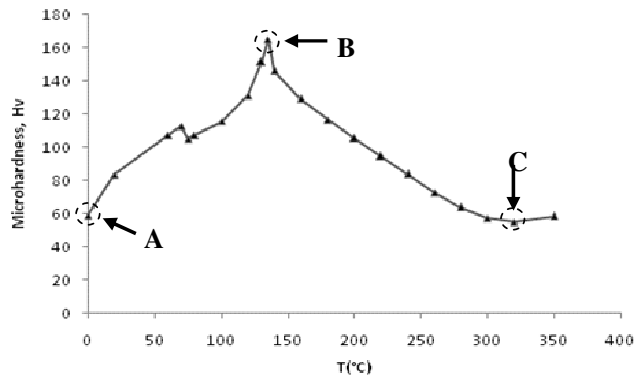
Fig. 1. Microhardness-temperature curve for the Al-4.6Zn-1.2Mg (wt %) aged for 2 h.

The microstructure of the three samples was examined by means of OM and the results are shown in Fig. 2. The present microstructures have equiaxed matrix grains. Significant grain growth was observed after heat treatment. Furthermore, one can observe some precipitates located on the interior of the grains and at grain boundaries. Detailed investigations of the different sample morphologies and the nature of the precipitates were carried out using SEM, EDX (Fig. 3) and TEM (Fig. 4). For the A-sample, one can notice two types of precipitates: the white precipitate displayed a remarkable content of Mg and Zn in its analysis, whereas the black one exhibited a high content of Fe and Si (Fig. 3A).
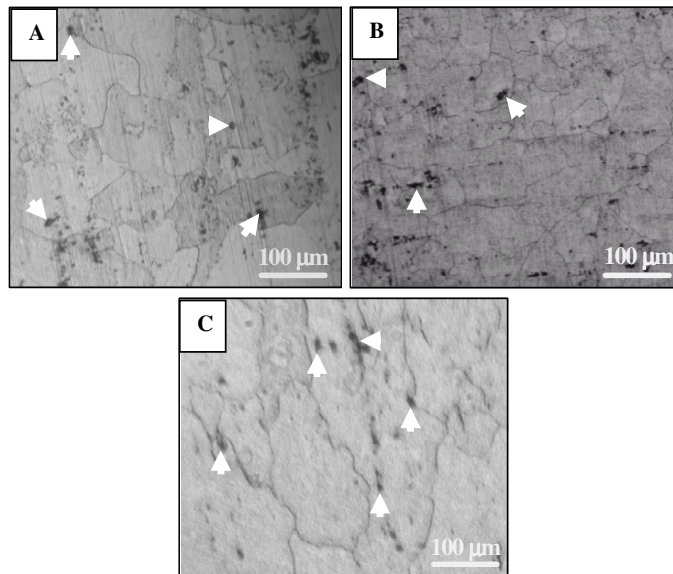

Fig. 2. OM micrographs of the selected samples A, B and C.

The SEM image of the B-sample shows that wide intermetallic precipitation occurred in the matrix and at the boundary (Fig. 3B), as already observed in optical micrographs. Precipitates have different dimensions: the smaller are coherent with the aluminium matrix whereas the larger ones are incoherent. The EDX analysis of these precipitates shows the presence of Mg and Zn elements. For the C-samples, one can observe the formation of the η-$MgZn_2$ phases (white precipitate) [21] and an increase in the black particles size (Fig. 3C).
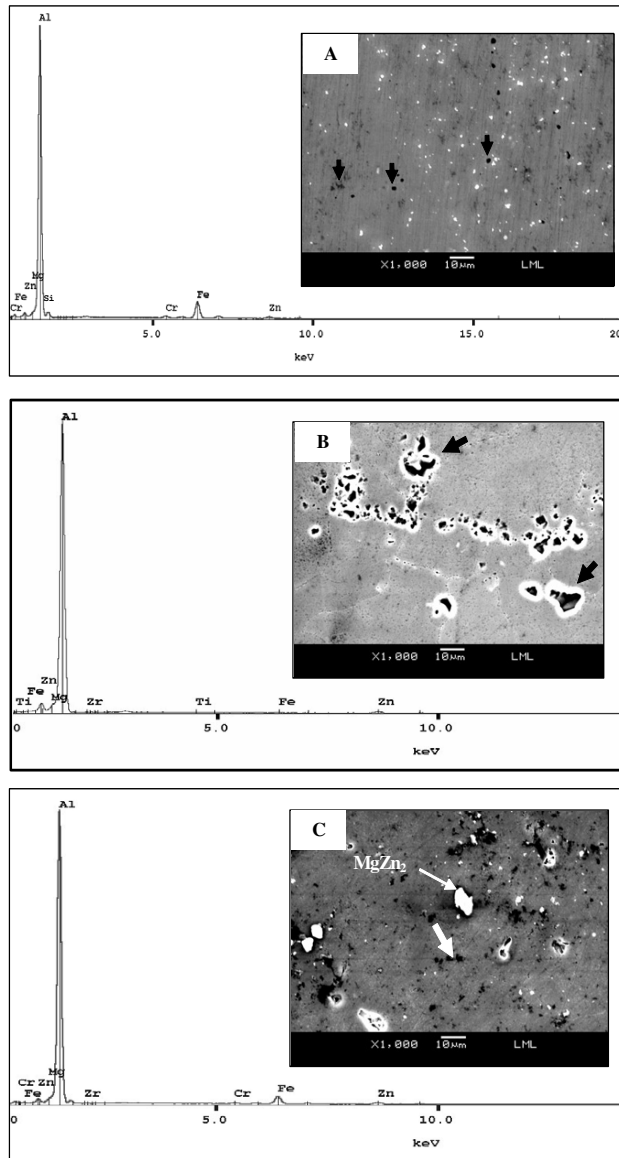
Fig. 3. SEM-images and the EDX analysis of the selected samples A, B and C

Figure 4 shows the TEM-images of the three samples. The size of particles observed in Al-Zn-Mg alloy by TEM depends very definitely on the temperature of annealing. As can be seen, the precipitates have different shapes: some (the smaller ones) were lath- like and some of polyhedral shaped (the larger ones). This difference could be ascribed to their growth being dependent on the matrix orientation. After quenching (Fig. 4A), the most numerous are the finest particles of a mean area of up to $11.8 \times 10^{-3} \mu m^2$. On the other hand, one can see larger particles having the Zr, Fe, Cr and Mn as main elements.

An interesting change in the sample B, correspondent to the one quenched and aged at 135°C took place, since a considerable increase in the content of the finest particles was observed, combined with a significant increase in particle sizes (Fig. 4B Zone 1). On the other hand, an examination of the same sample by TEM proved that a larger volume fraction of these precipitates were also located at grain boundaries (Fig. 4B Zone 2).

After quenching and ageing at 320°C (Fig. 3C and 4C), the content of the finest particles was decreased, whereas the larger ones were increased. On average, the mean of the larger particle observed under TEM was about $5\mu m^2$ and then remained rather stable, which suggested that particles of this type were primary, undissolved precipitates based on ferrous-manganese compounds [21].
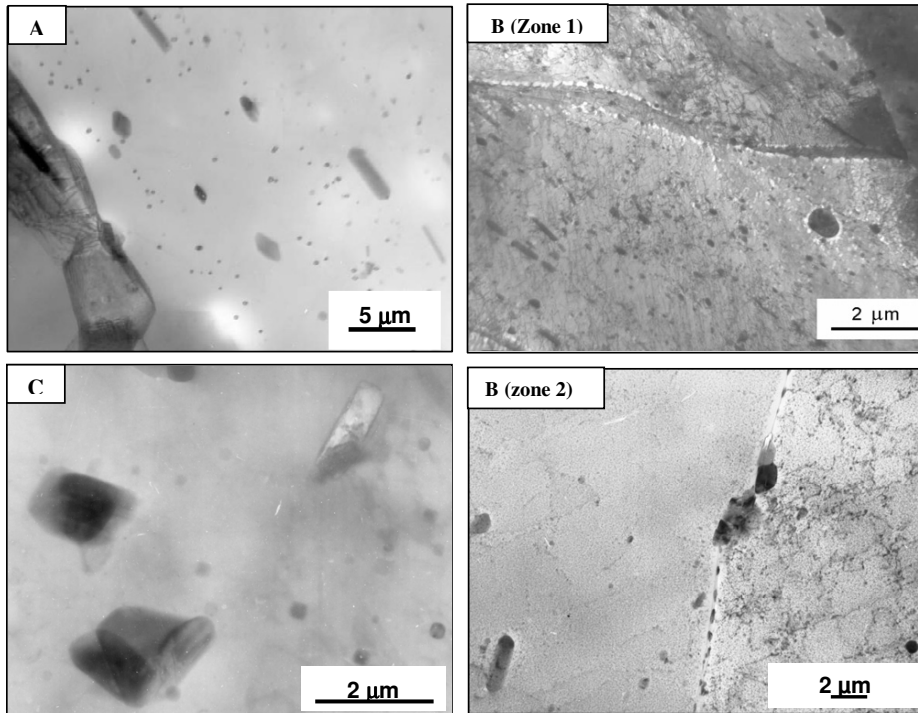

Fig. 4. TEM-images of the selected samples A, B(zone 1) and C and around grain boundaries of the sample B (zone 2).

Figure 5 displays the stress-strain curves of the investigated samples: A, B and C. The tensile test carried out just after quenching (sample A) showed the existence of the Portevin -Le Chatelier phenomenon. The material exhibited a good ductility of approximately 33% and yield strength of about 132 MPa. Although the increase in the yield strength could be accompanied by a reduction in the elongation, the A-sample, compared to the C one, has at the same time elevated values of the yield strength and elongation. This behaviour can be explained by the coalescence of the phases, i.e. iron and $MgZn_2$ precipitate, which are localised in the grain boundaries. This fact can give rise the embrittlement of the alloy. Compared to other metallurgical states, the tensile test of the B-sample exhibits the highest values of the yield strength (362 MPa), but at the expense of its elongation. This increase in yield stress can be attributed to the high density of the presence of the η'-phase.

The SEM-micrographs of the fracture surfaces corresponding to the tested samples A, B and C are also given in figure 5. The images of the three samples clearly indicate ductile fracture as characterized by the dimpled features. The ductile rupture starts on the particles (precipitates, inclusions) present in the alloy. Around these particles, the matrix becomes deformed plastically and in the direction of the deformation, one can note a separation particle-metal and thus the creation of small voids. In the present work, there is no fracture mode transition; however, as the

toughness decreases with increasing annealing temperatures, the voids produced change from being smaller and shallow (A sample) to large and deep (C sample). For the B sample, the increasing of the microhardness and the yield strength by η'-phase precipitation makes the specimen more brittle and there are occasionally what appear to be voids, left over from consolidation. Such residual microscale voids, although very rare in the specimen, may promote the initiation of shear localization and the onset of fracture.
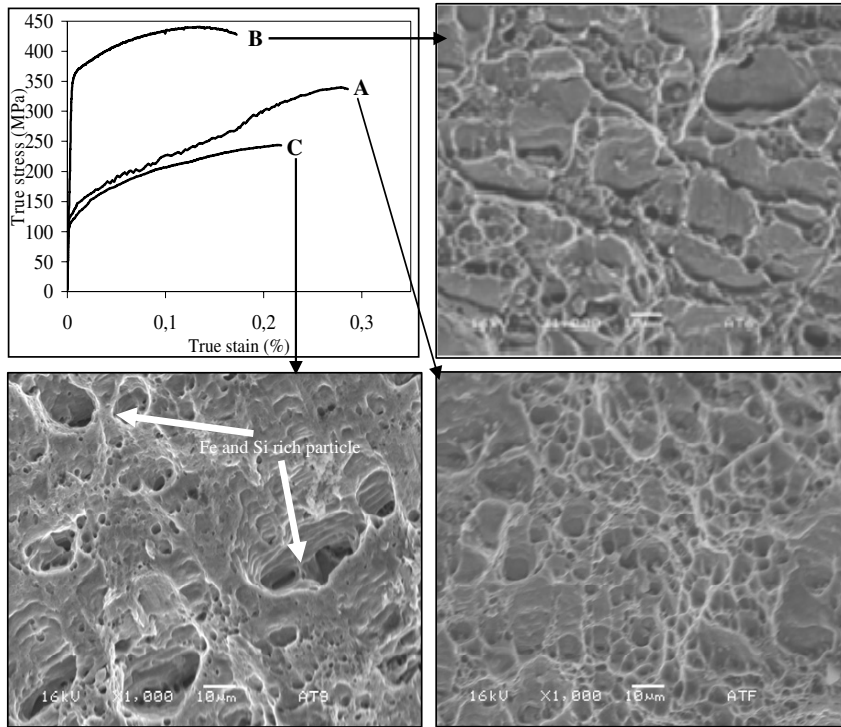

Fig. 5. Stress-strains curves and SEM-images of a typical fractographies after tensile tests of the selected samples: A, B and C.

In this work, the microindentation method was successfully employed to estimate the mechanical properties in the vicinity of fracture surfaces. Figure 6a shows the SEM-image of typical example of microindentation marks from the facture surfaces. The relationship between microindentation hardness and distance from the surface fracture is shown in figure 6b. Based on the direct observation of the microindentation marks, the hardness evolution of the A and C samples were found to be similar: with increasing the distance d, it is firstly observed that the microhardness monotonously decreases then, it becomes constant and takes the value of hardness obtained in the case of the investigated sample. The higher hardness values near the fracture surfaces can be explained by the creation of a plastic zone during the tensile test, whose dimensions are proportional to the strain hardening exponent (Table 2) of the investigated sample. While, in the case of the B sample, a remarkable increase in microhardness was observed towards fracture surface. This suggests that the η' precipitate dissolved in the region far from the surface fracture.
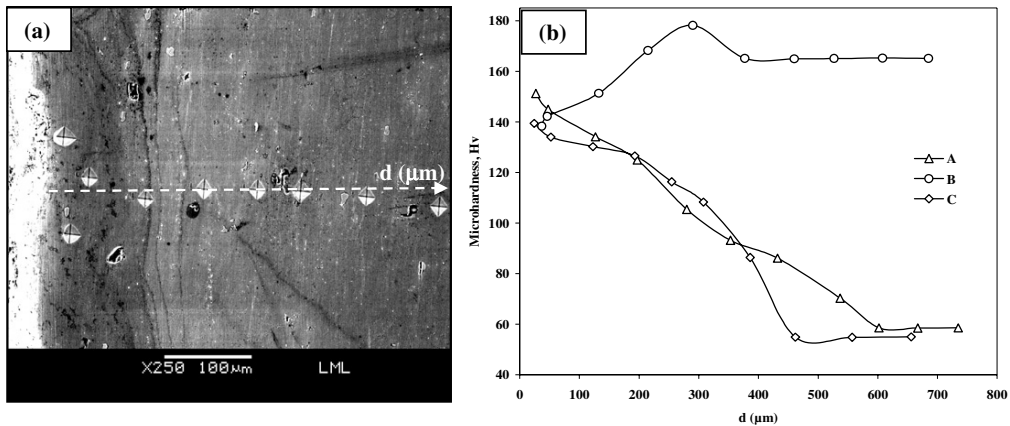
Fig. 6. (a) SEM-image of typical example of microindentation marks and (b) the measured values of Vickers hardness far from the fracture surface of the investigated samples.

Corresponding to the tensile tests shown in figure 7a, the TEM micrographs in figure 7b represents the microstructure of the sample obtained after two-step ageing treatment at 70°C (12h) and 135°C (8h). These TEM results also show that in our alloy the GP zone structure produced in the first step aging has strong effect on the size, distribution and density of η' phase particles formed in the subsequent aging at 135°C.

Tables 2 shows the results of mechanical properties measured of the A, B, C and the two steps treated samples. According to the hardness and yield strength values, one can deduce that the yield strength (Ys) monotonously varies with the hardness (Hv) and the (Ys/ Hv) quotient found almost constant (~2.2) for all the investigated samples. On the other hand, the strain hardening exponent (n), the deference between the tensile strength and yield strength (ΔS) and the elongation vary proportionately with the plastic zone dimensions.
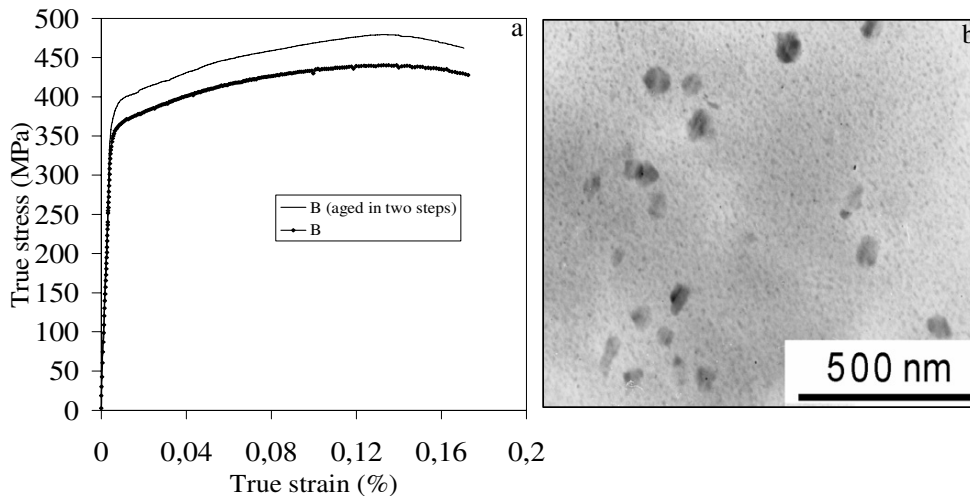

Fig. 7. (a)Stress-strains curves of B samples after one and two-step ageing and (b)TEM-image B sample after two-step ageing.

Table 2. Mechanical properties of the investigated Al-Mg-Zn alloy for different states.

	Hardness (Hv)	Yield Strength (MPa)	ΔS (MPa)	n	Elongation (%)	d (μm)
A	58.67	132.74	126.16	0.298	33.1	1204
B	165.04	362.32	31.86	0.083	18.82	754
C	54.89	116.68	81.32	0.216	24.34	924.2
Two-step	178.74	392.78	31.27	0.084	18.60	——

4. Conclusion

The effect of heat treatments on the microstructure and on the plastic properties of Al-Mg-Zn alloy has been investigated by different methods. The main experimental results and conclusions can be summarized as follows:

(i) After various states of ageing, the Al-Zn-Mg alloy shows significant changes in the microstructure and mechanical behaviour. After quenching, the microstructure was characterized by a high ductility, whereas the aged sample at 135°C, corresponding to the maximum value of hardness, revealed the presence of small η' precipitates.

(ii) The yield strength monotonously varies with the hardness. The ratio between these tow terms, was found almost constant (~2.2) for all the investigated samples. On the other hand, the strain hardening exponent (n), the deference between the tensile strength and yield strength (ΔS) and the elongation vary proportionately with the plastic zone dimensions.

(iii) Whatever the heat treatment, the samples rupture is considered a ductile mode. The ductility of B-sample is less pronounced with respect to other samples.

(iv) The microindentation method was successfully employed to estimate the mechanical properties in the vicinity of fracture surfaces: the behaviour of the A and C samples were found to be similar, whereas, in the case of the B sample, a remarkable increase in microhardness was observed towards fracture surface.

(v) After two-step ageing treatment, the specimen shows a fine distribution of η' precipitate. Compared to the B one, the two steps aged sample has a higher value of yield strength and the alloy retains its ductility.

Acknowledgements

References

[1] L.F. Mondolfo, Int. Metall. Rev. 153 (1971) 95.
[2] I.J. Polmear, "light Alloys", Metall. and Mater. Sci. Series, 3rd Edition, London (1995).
[3] J. Lendvai, Mater. Sci. Forum 43 (1996) 217-222.
[4] A. Deschamps, F. Livet and Y. Bréchet, Acta Mater 47 (1999) 281.
[5] P. Guyot and L. Cottignies, Acta Mater 44 (10) (1996) 4161-4167.
[6] J. C. Werenskiold and A. Deschamps, Mater Sci. Eng. A, Struct. Mater: Prop. Microstruc. Process 293 (2000)   267-274.
[7] J. D. Embury and A. Deschamps, Sc. Mater 49 (2003) 927-932.
[8] H. P. Degischer, W. Locom, A. Zahra and C. Y. Zahra, Z. Metallk 71 (1980) 231.
[9] L. K. Berg and J. GjØnnes, Acta Mater 49 (2001) 3443-3451.
[10] X. Z. Li, V. Hansen, Acta Mater 47(9) (1999) 2651-2659.
[11] S. K. Maloney, K. Hono, I.J. Polmear and S.P. Ringer, Micron 32 (2001) 741.
[12] H. Neuhauser and C. Schwin, Mat. Sci. and Technology, a comprehensive treatment (VCH, Weinheim) 88 (1993).
[13] D. J. Lloyd and D. Kenny, Metall. Trans. A13 (1982) 1445.
[14] A. D. Rollett, PhD thesis, Los Alamos National Laboratory USA. (1988).
[15] D. A. Hughes and W. D. Nix, Mat. Sci. Eng. A122 (1989) 153.
[16] A. Deschamps, Y. Brechet, C. J. Necker, S. Saimoto and J. D. Embury, Mat. Sci. Eng. A207 (1996) 143-152.
[17] Y. Estrin and L. P. Kubin, J. Mech. Beh. Mat. 2 (1989) 255.
[18] P. G. McCormick and Y. Estrin TMS 293 (1991).
[19] W. J. Poole, H. R. Shercliff, Mat. Sci. For. 1287 (1996) 217-222.
[20] C. H. Gür and Ì. Yildiz, Mat. Sci. and Eng A 382 (2004) 395-400.
[21] M. L. Grega, S. Hawrylkiewicz, M. Richert and W. Szymanski, Mat. Char. 46 (2001) 251-257.